arXiv:1603.05003v1 [quant-ph] 16 Mar 2016

Persistence of unvisited sites in quantum walks on a line

M. Štefaňák and I. Jex
Department of Physics, Faculty of Nuclear Sciences and Physical Engineering, Czech Technical University in Prague, Břehová 7, 115 19 Praha 1 - Staré Město, Czech Republic
(Dated: March 17, 2016)

We analyze the asymptotic scaling of persistence of unvisited sites for quantum walks on a line. In contrast to the classical random walk there is no connection between the behaviour of persistence and the scaling of variance. In particular, we find that for a two-state quantum walks persistence follows an inverse power-law where the exponent is determined solely by the coin parameter. Moreover, for a one-parameter family of three-state quantum walks containing the Grover walk the scaling of persistence is given by two contributions. The first is the inverse power-law. The second contribution to the asymptotic behaviour of persistence is an exponential decay coming from the trapping nature of the studied family of quantum walks. In contrast to the two-state walks both the exponent of the inverse power-law and the decay constant of the exponential decay depend also on the initial coin state and its coherence. Hence, one can achieve various regimes of persistence by altering the initial condition, ranging from purely exponential decay to purely inverse power-law behaviour.

PACS numbers: 03.67.-a,05.40.Fb,02.30.Mv

I. INTRODUCTION

Quantum walks [1–3] represent a versatile tool in quantum information processing with applications ranging from search algorithms [4–7], graph isomorphism testing [8–10], finding structural anomalies in graphs [11–13] or perfect state transfer [14–18]. Moreover, quantum walks were shown to be universal tools for quantum computation [19, 20].

One fundamental characterization of classical random walks on infinite lattices [21] is recurrence or transience. Random walk is said to be recurrent when the probability to return to the starting point at some later time (so-called Pólya number) is unity, and transient otherwise. In fact, recurrence ensures that any lattice point is visited with certainty. Pólya has shown [22] that for unbiased random walks this property depends on the dimension of the lattice. In particular, random walks are recurrent in dimensions 1 and 2 and transient on cubic and higher dimensional lattices. This result originates from the diffusive behaviour of a classical random walk.

Since measurement has a non-trivial effect on the state of the quantum system, one has to specify a particular measurement scheme to extend the concept of recurrence to the domain of quantum walks. One possibility is to consider a scheme [23] where the quantum walk is restarted from the beginning after the measurement, and in each iteration one additional step is performed. In this way the effect of measurement on the quantum state is minimized. Within this measurement scheme the Pólya number of a quantum walk depends not only on the dimension of the lattice, but also on the coin operator which drives the walk, and in some cases also on the initial coin state [24]. The ballistic nature of quantum walks implies that most of them are transient already in dimension 2. However, some quantum walks, such as the Grover walk [25–29], show the so-called trapping effect (or localization). This feature can be employed to construct recurrent quantum walks in arbitrary dimension [24].

Another scheme is to continue with the quantum walk evolution after the measurement [30]. The effect of frequent measurement is that the quantum walks are transient already on a one-dimensional lattice, as follows from [31]. Recurrence of quantum state within this measurement scheme has been analyzed for general discrete time unitary evolution in [32]. The authors have found that the expectation value of the first return time is quantized, i.e. it is either infinite or an integer. More recently, it was shown [33] that this property is preserved even in iterated open quantum dynamics, provided that the corresponding superoperator is unital in the relevant part of the Hilbert space. Moreover, the notion of monitored recurrence was extended to a finite-dimensional subspace in [34]. In such case the averaged expected return time is a rational number.

Persistence describes the probability that a given site remains unvisited until certain number of steps. As such, it can be viewed as a complementary event to that of recurrence. For classical random walks on a line and a plane persistence of any site tends to zero for large number of steps. In particular, on one-dimensional lattice persistence obeys an inverse power-law with exponent 1/2, which follows in a straightforward way from the diffusive behaviour of a random walk [35].

In the context of quantum walks persistence was first introduced in [36]. The authors have analyzed persistence for two-state Hadamard walk on a line within the measurement scheme of [23], i.e. when the quantum walk is restarted after the measurement. It was found that persistence of any site follows an inverse power-law with exponent determined numerically as $\lambda \approx 0.318$. In contrast to the classical case, no clear connection of the exponent to the spreading properties of the quantum walk was found.

In the present paper we give analytical explanation of

the results found in [36]. The study of persistence is extended to a one-parameter set of two-state quantum walks on a line. We confirm that persistence obeys an inverse power-law. The exponent is determined solely by the parameter of the coin operator. Hence, there is no connection of the exponent to the scaling of variance like in the classical random walk. Moreover, we analyze persistence of sites for a set of three-state quantum walks [37–39] which involves the familiar Grover walk [26–28] as a special case. We find that persistence exhibits a more complicated asymptotic behaviour. In addition to the inverse power-law there is also an exponential decay which arises from the trapping effect. The analytical results are obtained using the suitable basis of the coin space formed by the eigenvectors of the coin operator [39]. Both the exponent of the inverse power-law and the decay rate of the exponential decay depend on the coin parameter and, in contrast to the two-state walk, on the initial coin state and its coherence. Hence, it is possible to obtain various regimes of persistence, ranging from pure inverse power-law to pure exponential decay, by choosing different initial condition. Moreover, we find that for some initial coin states persistence behave differently for lattice sites on the positive and negative half-lines.

The paper is organized as follows: In Section II we review the definition of persistence of site m within a particular measurement scheme of [23, 36]. We provide an estimate of the asymptotic behaviour of persistence based on the limit density. Section III is dedicated to the analysis of persistence in two-state quantum walks. In Section IV we perform similar analysis for a set of three-state quantum walks. More technical details are left for Appendices A and B. We conclude and present an outlook in Section V.

II. PERSISTENCE OF UNVISITED SITES

In this Section we briefly introduce persistence of a given site and provide and estimate of its asymptotic behaviour. We follow the measurement scheme used in [23, 36], where the quantum walk is restarted from the beginning after each measurement. By persistence of a site m we understand the probability that the particular lattice point remains unvisited until T steps. Since the walk starts at the origin of the lattice we only consider persistence of sites $m \neq 0$. We find that this probability is given by [36]

$$\mathcal{P}_m(T) = \prod_{t=1}^{T}(1 - p(m,t)), \tag{1}$$

where $p(m,t)$ denotes the probability to find the quantum particle at position m after t steps of the quantum walk.

Let us now turn to the approximation of persistence for large T. For this purpose we re-write (1) in the exponential form

$$\begin{aligned}\mathcal{P}_m(T) &= \exp\left(\ln\left(\prod_{t=1}^{T}(1 - p(m,t))\right)\right)\\ &= \exp\left(\sum_{t=1}^{T}\ln(1 - p(m,t))\right).\end{aligned}$$

We replace the logarithm by the first order Taylor expansion and arrive at

$$\mathcal{P}_m(T) \approx \exp\left(-\sum_{t=1}^{T} p(m,t)\right). \tag{2}$$

Next, we use the limit density $w(v)$ derived from the weak-limit theorem [40] to estimate the exact probability $p(m,t)$ by

$$p(m,t) \approx \frac{1}{t} w\left(\frac{m}{t}\right).$$

Finally, we estimate the sum in (2) with an integral

$$\mathcal{I}_m(T) = \int_1^T \frac{1}{t} w\left(\frac{m}{t}\right) dt \tag{3}$$

and obtain the approximation of persistence

$$\mathcal{P}_m(T) \approx \exp\left(-\mathcal{I}_m(T)\right). \tag{4}$$

In the following we analyze persistence of unvisited sites for two- and three-state quantum walks on a line. Detailed evaluations of the integral (3) are left for the Appendices.

III. TWO-STATE WALK ON A LINE

Let us start our analysis with the two-state quantum walk on a line with the coin operator

$$C(\rho) = \begin{pmatrix} \rho & \sqrt{1-\rho^2} \\ \sqrt{1-\rho^2} & -\rho \end{pmatrix}, \quad 0 < \rho < 1.$$

The coin parameter ρ determines the speed of propagation of the wave packet on the line [41]. For $\rho = 1/\sqrt{2}$ we obtain the familiar Hadamard walk [31].

Suppose that the initial coin state of the particle was

$$|\psi_C\rangle = a|L\rangle + b|R\rangle.$$

The limiting probability density for the two-state quantum walk is given by [42, 43]

$$w(v) = \frac{\frac{\sqrt{1-\rho^2}}{\rho}\left(1 - v\Lambda(a,b)\right)}{\pi\left(1 - v^2\right)\sqrt{1 - \frac{v^2}{\rho^2}}},$$

where Λ is determined by the initial coin state and the coin parameter

$$\Lambda(a,b) = |a|^2 - |b|^2 + \frac{\sqrt{1-\rho^2}}{\rho}\left(a\bar{b} + b\bar{a}\right).$$

Before we turn to the persistence we first simplify the dependence on the initial coin state Λ by changing the basis of the coin space. Following the idea of [44] we consider the basis formed by the eigenvectors of the coin operator

$$\begin{aligned} |\chi^+\rangle &= \sqrt{\frac{1+\rho}{2}}|L\rangle + \sqrt{\frac{1-\rho}{2}}|R\rangle, \\ |\chi^-\rangle &= -\sqrt{\frac{1-\rho}{2}}|L\rangle + \sqrt{\frac{1+\rho}{2}}|R\rangle, \end{aligned} \tag{5}$$

which satisfy the relations

$$C(\rho)|\chi^\pm\rangle = \pm|\chi^\pm\rangle.$$

We decompose the initial coin state of the walk into the eigenvector basis as

$$|\psi_C\rangle = h_+|\chi^+\rangle + h_-|\chi^-\rangle.$$

From (5) we find that the coefficients of the initial coin state in the standard basis a and b are related to the eigenbasis coefficients $h_\pm$ by

$$\begin{aligned} a &= \frac{\sqrt{1+\rho}}{\sqrt{2}}h_+ - \frac{\sqrt{1-\rho}}{\sqrt{2}}h^-, \\ b &= \frac{\sqrt{1-\rho}}{\sqrt{2}}h_+ + \frac{\sqrt{1+\rho}}{\sqrt{2}}h^-. \end{aligned}$$

In the new basis the factor $\Lambda(a,b)$ becomes

$$\Lambda(h_+,h_-) = \frac{2|h_+|^2 - 1}{\rho}.$$

The asymptotic probability density thus simplifies into

$$w(v) = \frac{\frac{\sqrt{1-\rho^2}}{\rho}\left(1 - \frac{v}{\rho}(2|h_+|^2 - 1)\right)}{\pi\left(1-v^2\right)\sqrt{1-\frac{v^2}{\rho^2}}} \tag{6}$$

Let us now turn to persistence. We leave the details of evaluation of the integral (4) for Appendix A. We find that for large T the function $\mathcal{I}_m(T)$ grows like a logarithm

$$\mathcal{I}_m(T) \sim \lambda \ln\left(\frac{T}{|m|}\right),$$

where the pre-factor reads

$$\lambda = \frac{\sqrt{1-\rho^2}}{\rho\pi}. \tag{7}$$

Hence, we find that in the asymptotic regime persistence of site m follows an inverse power-law

$$\mathcal{P}_m(T) \sim \left(\frac{T}{|m|}\right)^{-\lambda}, \tag{8}$$

The exponent λ is independent of the initial coin state. It is determined solely by the coin operator, i.e. by the value of ρ. Note that for $\rho = 1/\sqrt{2}$, i.e. the Hadamard walk, we find that $\lambda = \frac{1}{\pi} \approx 0.318$, which is in agreement with the numerical result obtained in [36].

Our results are illustrated in Figures 1-3. In Figure 1 we show the influence of the initial coin state. In the first two plots we display the probability distribution of the two-state quantum walk with the coin parameter $\rho = 1/\sqrt{2}$, i.e. the Hadamard walk. In all Figures grey circles represent the data-points obtained from numerical simulation. The red curves correspond to the asymptotic probability density given by (6). For the upper plot we have chosen the initial coin state $|\psi_C^{(1)}\rangle = |\chi^-\rangle$. The resulting probability density shows only one peak on the right. In the middle plot the initial coin state was chosen according to $|\psi_C^{(2)}\rangle = \frac{1}{\sqrt{2}}\left(|\chi^+\rangle + |\chi^-\rangle\right)$. This state leads to a symmetric distribution. Despite the differences in the probability distributions the persistence shows the same asymptotic scaling, as we illustrate in the last figure. Here we display the persistence of site $m = 2$ as a function of the number of steps T. To unravel the inverse power-law behavior we use log-log scale. The grey circles correspond to the numerical simulation and the red curves show the inverse power-law (8).

In Figure 2 we illustrate the influence of the coin parameter ρ. In the first two plots we show the probability distribution of the two-state quantum walk with the initial coin state $|\psi_C\rangle = \frac{1}{\sqrt{2}}(|\chi^+\rangle + |\chi^-\rangle)$. For the upper plot the coin parameter is $\rho_1 = 0.2$. In the middle plot we have chosen the coin parameter $\rho_2 = 0.8$. We see that the coin parameter directly affects the speed at which the walk spreads through the lattice [41]. The lower plot shows the difference in the scaling of persistence of site $m = 2$ for different values of ρ. We use log-log scale to unravel the scaling of persistence. We find that the exponent of the inverse power-law decreases with increasing value of ρ, in accordance with (7).

Finally, Figure 3 illustrates that the asymptotic behaviour of persistence is independent of the actual position m. The upper plot displays the probability distribution of the two-state walk with coin parameter $\rho = 0.5$ and the initial coin state $|\psi_C\rangle = |\chi^+\rangle$. This initial condition leads to a density which is the most biased towards left, as indicated by the presence of only one peak. In the lower plot we show persistence of sites $m = 2$ and $m = -2$ on a log-log scale. Despite the differences in the intermediate regime, the slope of both curves is the same, in agreement with (8).

To conclude this Section, we have found that for the two-state quantum walk on a line persistence of unvisited sites obeys an inverse power-law (8) with exponent (7) determined only by the coin parameter.

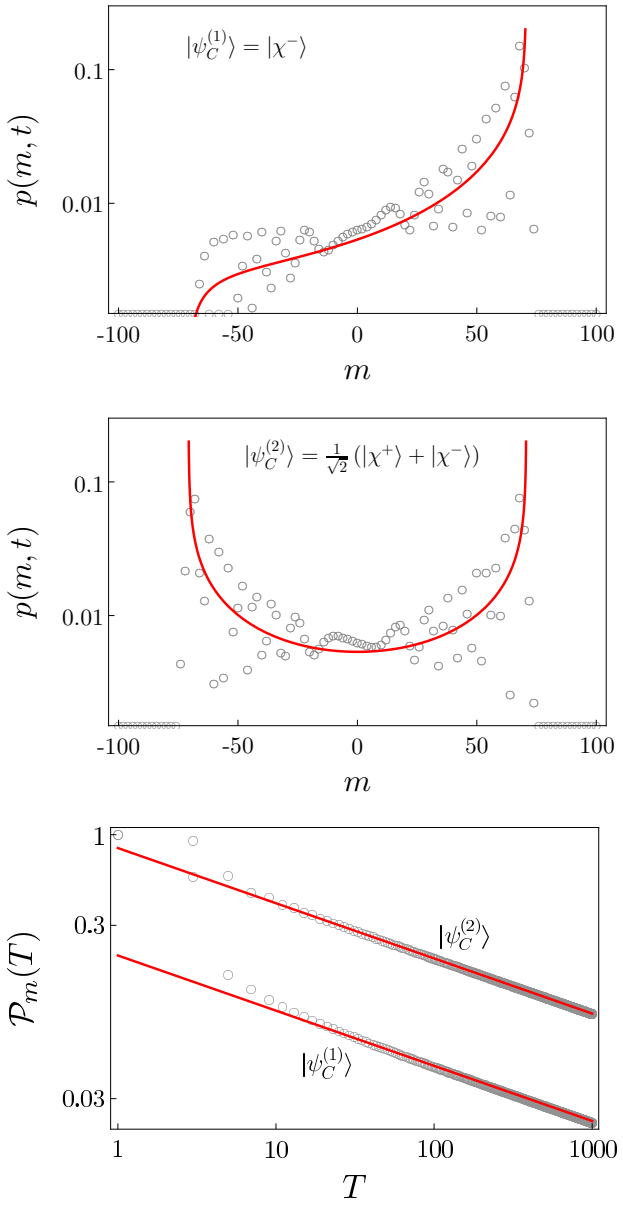

FIG. 1. Probability density and persistence in dependence on the choice of the initial coin state for the Hadamard walk ($\rho = 1/\sqrt{2}$). The first two plots show the probability distribution of the Hadamard walk after $t = 100$ steps for two different initial coin states $|\psi_C^{(1,2)}\rangle$ on a semi-log scale. In the lower plot we display persistence of site $m = 2$ as a function of the number of steps T on a log-log scale. Despite the differences in the probability distributions the asymptotic scaling of persistence is independent of the initial state, in accordance with (8).

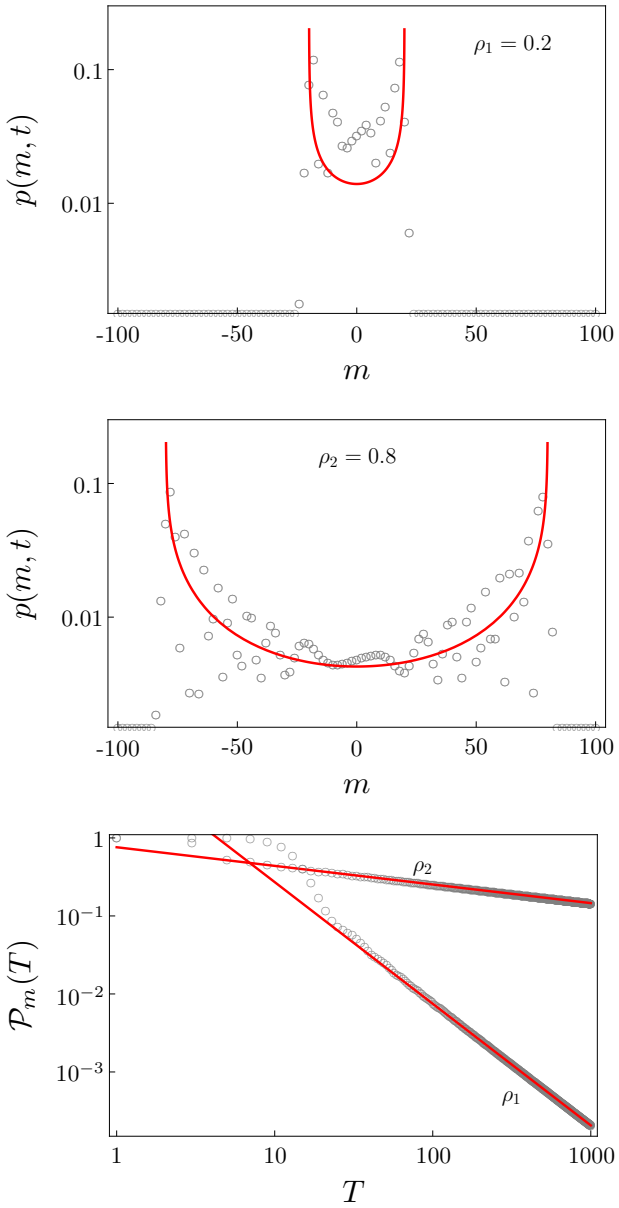

FIG. 2. Probability density and persistence in dependence on the choice of the coin parameter ρ. The first two plots show the probability distribution of the two-state quantum walk on a semi-log scale. In both situations the initial coin state was chosen as $|\psi_C\rangle = \frac{1}{\sqrt{2}}(|\chi^+\rangle + |\chi^-\rangle)$, which leads to symmetric probability distribution. In the upper plot the coin parameter is $\rho_1 = 0.2$ while in the middle plot we have chosen $\rho_2 = 0.8$. The lower plot shows scaling of persistence of site $m = 2$ for different values of $\rho_{1,2}$ on a log-log scale. The exponent of the inverse power-law (8) decreases with increasing value of ρ, as predicted by (7).

IV. THREE-STATE WALK ON A LINE

Let us now turn to the three-state walk on a line. Here the particle is allowed to move to the left, stay at its position or move to the right. We denote the corresponding orthogonal coin states by $|L\rangle$, $|S\rangle$ and $|R\rangle$. As for the coin operator we consider the one which was studied in [37–39]. In the standard basis $\{|L\rangle, |S\rangle, |R\rangle\}$ the coin operator is given by the matrix

$$C(\rho) = \begin{pmatrix} -\rho^2 & \rho\sqrt{2-2\rho^2} & 1-\rho^2 \\ \rho\sqrt{2-2\rho^2} & 2\rho^2-1 & \rho\sqrt{2-2\rho^2} \\ 1-\rho^2 & \rho\sqrt{2-2\rho^2} & -\rho^2 \end{pmatrix}, \quad (9)$$

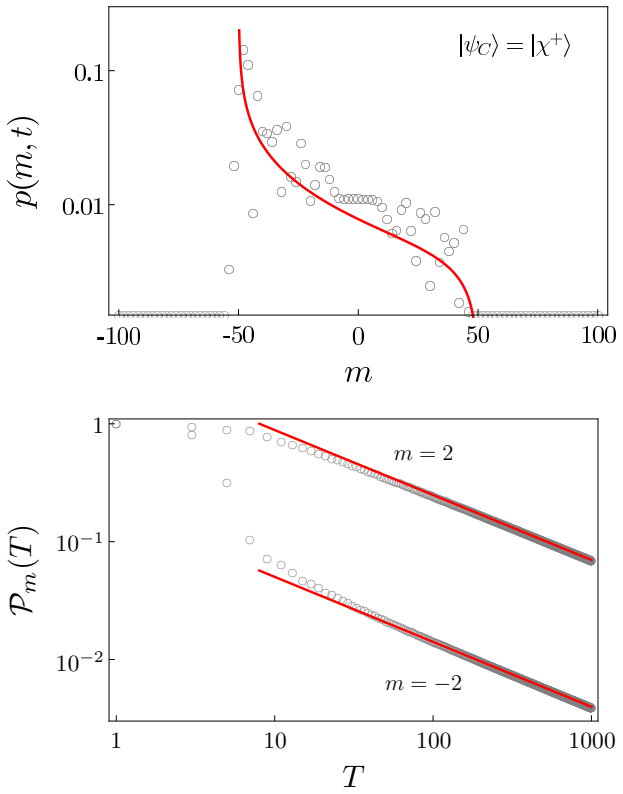

FIG. 3. The first plot shows the probability distribution for the two-state walk with $\rho = 0.5$. The initial coin state is $|\psi_C\rangle = |\chi^+\rangle$, which results in density with only one peak on the left. The lower plot illustrates the behaviour of persistence of sites $m = 2$ and $m = -2$. Both curves have the same slope (7) which is determined solely by the coin parameter ρ.

with parameter $\rho \in (0, 1)$. Quantum walks with such a coin operator represent a one-parameter extension of the familiar three-state Grover walk [26–28], which corresponds to the choice of $\rho = 1/\sqrt{3}$. Indeed, the results of [39] have shown that the considered quantum walks share the same features and the coin factor ρ is a scaling parameter which determines the rate of spreading of the three-state quantum walk across the line.

To evaluate persistence of unvisited sites we estimate the exact probability distribution $p(m, t)$ for large number of steps t. In contrast to the two-state walk, the properties of the probability distribution are not fully captured by the limit density $w(v)$. Indeed, the three-state quantum walk leads to the trapping effect [26–28, 38, 39], which means that the probability of finding the particle at position m has a non-vanishing limit for t approaching infinity. We denote the limiting value

$$\lim_{t\to\infty} p(m,t) = p_\infty(m),$$

as the trapping probability. Hence, for large t we approximate the probability to find the particle at position m at time t with the sum

$$p(m,t) \approx \frac{1}{t} w\left(\frac{m}{t}\right) + p_\infty(m).$$

The limit density $w(v)$ and the trapping probability $p_\infty(m)$ were analyzed in [38, 39]. We follow the results of [39] since they have simpler form due to the use of a more suitable basis of the coin space. In particular, the basis of the coin space was constructed from the eigenvectors of the coin operator (9) which reads

$$\begin{aligned}
|\sigma^+\rangle &= \sqrt{\frac{1-\rho^2}{2}}|L\rangle + \rho|S\rangle + \sqrt{\frac{1-\rho^2}{2}}|R\rangle,\\
|\sigma_1^-\rangle &= \frac{\rho}{\sqrt{2}}|L\rangle - \sqrt{1-\rho^2}|S\rangle + \frac{\rho}{\sqrt{2}}|R\rangle,\\
|\sigma_2^-\rangle &= \frac{1}{\sqrt{2}}(|L\rangle - |R\rangle).
\end{aligned}$$

The vectors satisfy the eigenvalue equations

$$C(\rho)|\sigma^+\rangle = |\sigma^+\rangle, \qquad C(\rho)|\sigma_i^-\rangle = -|\sigma_i^-\rangle, i = 1, 2.$$

We decompose the initial coin state into the eigenstate basis according to

$$|\psi_C\rangle = g_+|\sigma^+\rangle + g_1|\sigma_1^-\rangle + g_2|\sigma_2^-\rangle.$$

The limiting probability density then reads [39]

$$w(v) = \frac{\sqrt{1-\rho^2}}{\pi(1-v^2)\sqrt{\rho^2-v^2}}\left(1 - |g_2|^2 - \right. \qquad (10)$$
$$\left. -(g_1\overline{g_2} + \overline{g_1}g_2)\frac{v}{\rho} + (|g_2|^2 - |g_+|^2)\frac{v^2}{\rho^2}\right).$$

The trapping probability is given by [39]

$$p_\infty(m) = \begin{cases} \frac{2-2\rho^2}{\rho^4}Q^{2m}|g_+ + g_2|^2, & m > 0,\\ \frac{Q}{\rho^2}\left\{|g_+|^2 + (1-\rho^2)|g_2|^2\right\}, & m = 0,\\ \frac{2-2\rho^2}{\rho^4}Q^{2|m|}|g_+ - g_2|^2, & m < 0 \end{cases} \qquad (11)$$

where Q depends on the coin parameter ρ

$$Q = \frac{2-\rho^2-2\sqrt{1-\rho^2}}{\rho^2}.$$

Let us estimate the persistence of site m. We approximate the sum in (2) with

$$\sum_{t=1}^{T} p(m,t) \approx \mathcal{I}_m(T) + \sum_{t=\left\lceil\frac{|m|}{\rho}\right\rceil}^{T} p_\infty(m),$$

where $\mathcal{I}_m(T)$ is defined in (3). The sum on the right hand side is trivial

$$\sum_{t=\left\lceil\frac{|m|}{\rho}\right\rceil}^{T} p_\infty(m) = \left(T - \left\lceil\frac{|m|}{\rho}\right\rceil\right) p_\infty(m).$$

Here $\lceil x\rceil$ denotes the ceiling of x, i.e. the smallest integer not less than x. The integral $\mathcal{I}_m(T)$ is evaluated in

Appendix B. We find that $\mathcal{I}_m(T)$ asymptotically grows like a logarithm

$$\mathcal{I}_m(T) \sim \lambda \ln\left(\frac{T}{|m|}\right),$$

where the pre-factor reads

$$\lambda = \frac{\sqrt{1-\rho^2}}{\pi\rho}\left(1-|g_2|^2\right).$$

We conclude that for the three-state quantum walk on a line persistence of site m behaves asymptotically like

$$\mathcal{P}_m(T) \sim \left(\frac{T}{|m|}\right)^{-\lambda} e^{-p_\infty(m)T}. \tag{12}$$

We see that there are two contributions to persistence. Similarly to the two-state walk there is an inverse power-law. In addition, the trapping effect contributes with the exponential decay. However, the behavior of persistence depends on the initial state, in contrast to the two-state walk. Indeed, both λ and the trapping probability $p_\infty(m)$ are determined by the initial condition. The exponent λ depends only on the probability $|g_2|^2$ to find the initial coin state $|\psi_C\rangle$ in the eigenstate $|\sigma_2^-\rangle$. On the other hand, the rate of the exponential decay is determined by the interference of the amplitudes g_+ and g_2. In the following we discuss various initial conditions to illustrate our result.

Let us first consider the initial coin state $|\psi_C\rangle = |\sigma^+\rangle$. In such a case the general formula (12) for the asymptotic behaviour of persistence turns into

$$\mathcal{P}_m^{(g_+)}(T) \sim \left(\frac{T}{|m|}\right)^{-\lambda} e^{-\gamma(m)T}, \tag{13}$$

with the exponent given by

$$\lambda = \frac{\sqrt{1-\rho^2}}{\pi\rho}, \tag{14}$$

and the decay constant

$$\gamma(m) = \frac{2(1-\rho^2)}{\rho^4} Q^{2|m|}. \tag{15}$$

We see that both contributions, namely the inverse power-law and the exponential decay, are present. For illustration of this result, we show in Figure 4 the probability distribution and persistence for the three-state walk with the coin parameter $\rho = 0.8$. The first plot displays the probability distribution after $t = 100$ steps. The grey circles corresponds to the numerical simulation, the red curve depicts the asymptotic probability density (10) and the blue dashed curve corresponds to the trapping probability (11). The second plot illustrates persistence of sites $m = 2$ and $m = 10$ on the log-log scale. For $m = 2$ the decay of persistence is faster than inverse power-law. Indeed, for large number of steps the exponential decay starts to play a dominant role. On the other hand, for $m = 10$ we do not observe any deviation from the inverse power-law at the considered time-scale. This is due to the fact that the decay constant (15) itself decreases exponentially with the distance from the origin. The last plot, where we display persistence of site $m = 2$ on the logarithmic scale, illustrates that $\mathcal{P}_m(T)$ decays exponentially in the long-time limit.

Let us now turn to the initial coin state $|\psi_C\rangle = |\sigma_2^-\rangle$. The general formula for persistence of site m (12) for $g_2 = 1$ reduces into purely exponential decay

$$\mathcal{P}_m^{(g_2)}(T) \sim e^{-\gamma(m)T}, \tag{16}$$

where the decay rate $\gamma(m)$ is given by (15). To illustrate this effect, we display in Figure 5 the probability distribution and persistence for the Grover walk, i.e. $\rho = 1/\sqrt{3}$. The first plot shows the probability distribution after $t = 100$ steps. The second plot displays persistence of sites $m = 1$, $m = 2$ and $m = 5$. The decay rate (15) decreases exponentially with the growing distance from the origin. Hence, already for $m = 5$ persistence essentially saturates on the considered time-scale. The last plot shows persistence of site $m = 2$ on a log-scale. The figure illustrates that the decay of persistence is indeed purely exponential.

Next, we consider the initial coin state $|\psi_C\rangle = |\sigma_1^-\rangle$. In such a case the expression (12) reduces to a pure inverse power-law

$$\mathcal{P}_m^{(g_1)}(T) \sim \left(\frac{T}{|m|}\right)^{-\lambda}, \tag{17}$$

with the exponent λ given by (14). To illustrate this feature, we show in Figure 6 the probability distribution and persistence for the three-state walk with the coin parameter $\rho = 0.6$. The upper plot displays the probability distribution after 100 steps. We find that for the particular initial state $|\psi_C\rangle = |\sigma_1^-\rangle$ the trapping effect disappears. Indeed, according to (11) we find that $p_\infty(m)$ vanishes if $g_+ = g_2 = 0$. The lower plot displays persistence of sites $m = 2$ and $m = 5$. The log-log scale unravels that the scaling is given only by the inverse power-law (17).

Finally, let us point out that the dependence of the trapping probability (11) on the initial coin state can be different for positive and negative m. This leads to different behavior of persistence for sites on positive and negative half-lines. As an example, consider the initial coin state

$$|\psi_C\rangle = \frac{1}{\sqrt{2}}\left(|\sigma^+\rangle + |\sigma_2^-\rangle\right). \tag{18}$$

We find that persistence of sites on positive half-line ($m > 0$) behaves like

$$\mathcal{P}_m^+(T) \sim \left(\frac{T}{m}\right)^{-\lambda} e^{-\gamma(m)T}, \tag{19}$$

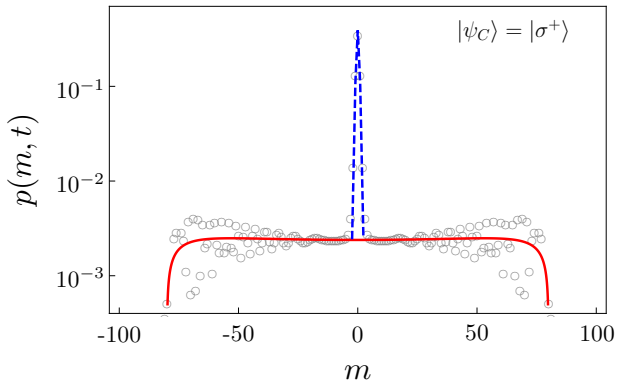

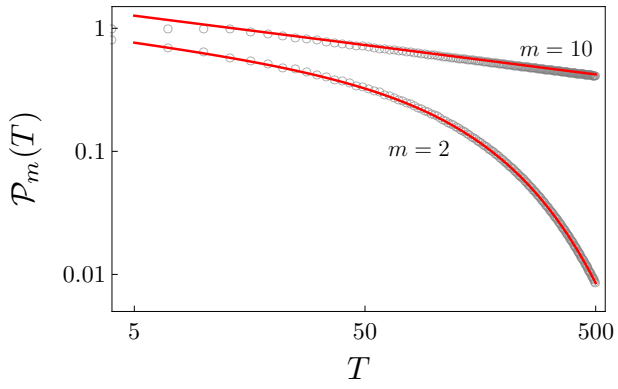

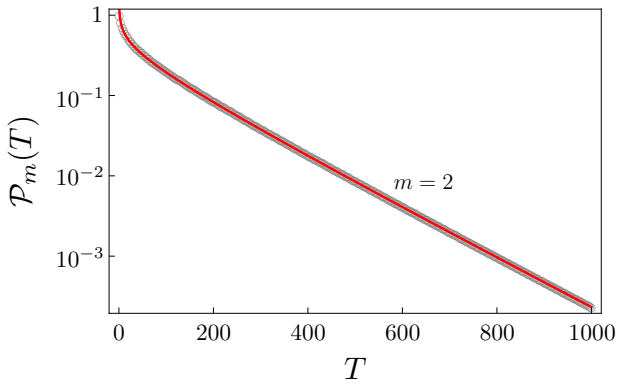

FIG. 4. Probability distribution and persistence for the three-state walk with $\rho = 0.8$ starting with the coin state $|\psi_C\rangle = |\sigma^+\rangle$. In the first plot we show the probability distribution after $t = 100$ steps. The second plot displays persistence (13) of sites $m = 2$ and $m = 10$ on the log-log scale. For $m = 2$ the decay of persistence is faster than the inverse power-law. The deviation is due to the exponential decay which starts to play a dominant role for large T. We do not observe this effect for $m = 10$, since the decay constant decreases exponentially with the distance from the origin. The third plot, which shows persistence of site $m = 2$ on the log-scale, confirms that $\mathcal{P}_m(T)$ decays exponentially.

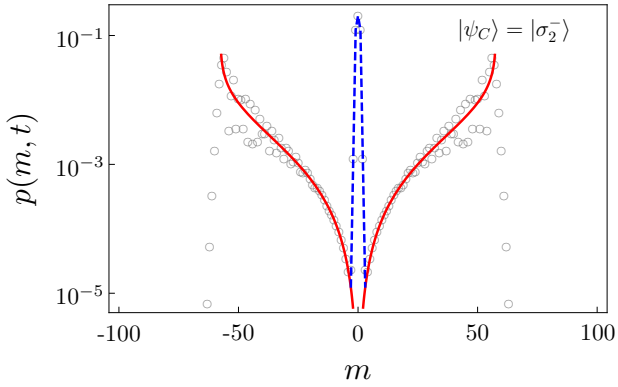

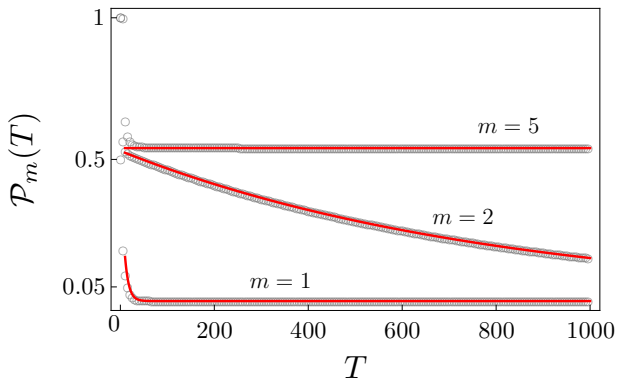

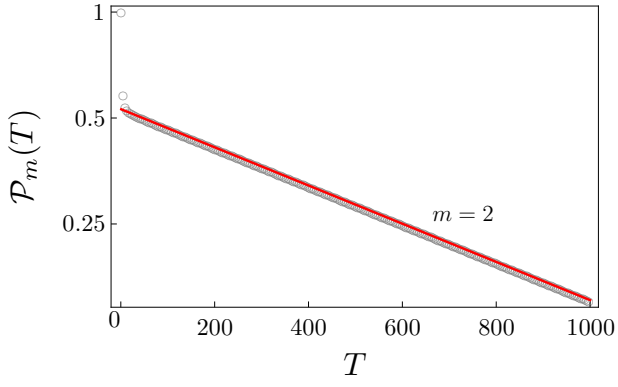

FIG. 5. Probability distribution and persistence for the three-state Grover walk starting with the coin state $|\psi_C\rangle = |\sigma_2^-\rangle$. In the upper plot we show the probability distribution after $t = 100$ steps. The middle plot displays persistence (16) of sites $m = 1$, $m = 2$ and $m = 5$. The decay is exponential but the rate drops down very fast with the growing distance from the origin. The lower plot with the log-scale on the y-axis illustrates that the decay of persistence is indeed purely exponential (16).

where the exponent reads

$$\lambda = \frac{\sqrt{1-\rho^2}}{2\pi\rho}, \tag{20}$$

and the decay rate is given by

$$\gamma(m) = \frac{4(1-\rho^2)}{\rho^4} Q^{2m}.$$

Hence, for positive m persistence decays exponentially in the asymptotic regime. However, for sites on the negative half-line ($m < 0$) persistence obeys only the inverse

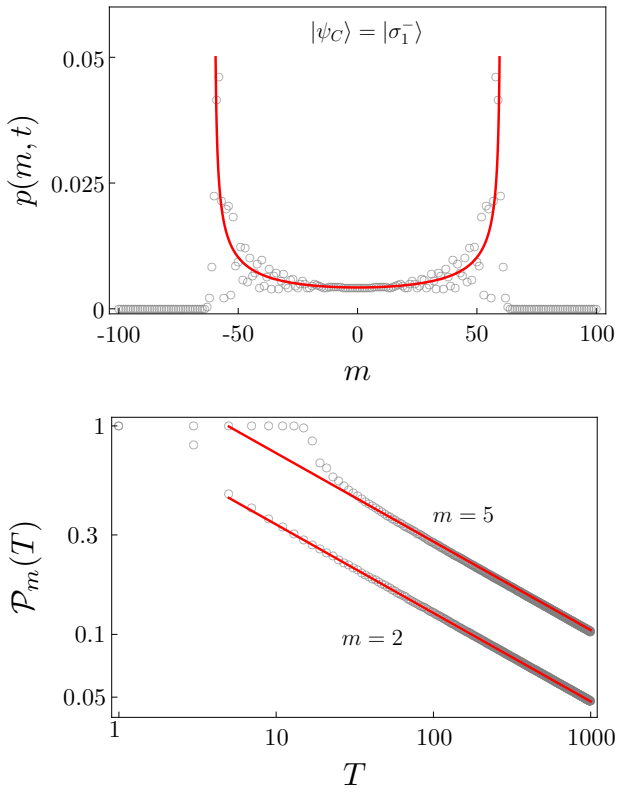

FIG. 6. Probability distribution and persistence for the three-state walk with $\rho = 0.6$ starting with the coin state $|\psi_C\rangle = |\sigma_1^-\rangle$. The upper plot shows the probability distribution after $t = 100$ steps. For this particular initial state the trapping effect disappears. The lower plot displays persistence of sites $m = 2$ and $m = 5$ on a log-log scale. We find that the scaling is given by the inverse power-law (17).

power-law

$$\mathcal{P}_m^-(T) \sim \left(\frac{T}{|m|}\right)^{-\lambda}, \tag{21}$$

with the exponent λ given by (20). We point out that coherence of the initial coin state is crucial for this effect. Indeed, consider the initial coin state given by an incoherent mixture of the basis states

$$\rho_C = \frac{1}{2}|\sigma^+\rangle\langle\sigma^+| + \frac{1}{2}|\sigma_2^-\rangle\langle\sigma_2^-|.$$

In such a case persistence is given by the sum of the expressions (16) and (17) with the corresponding exponent (14) and decay rate (15), independent of the sign of the position m. Hence, there is no asymmetry between negative and positive m and persistence of all lattice sites decays exponentially in the asymptotic regime. Compared to the coherent superposition (18) the exponent (14) is larger by a factor of two while the decay rate (15) is smaller by a factor of two.

We illustrate the results for the initial coin state (18) in Figure 7 where we consider the three-state quantum walk with the coin parameter $\rho = 0.5$. In the upper plot we display the probability distribution after 100 steps of the walk. Notice that the trapping probability, highlighted by the dashed blue curve, is non-zero only on the positive half-line. The lower plot illustrates the difference in the scaling of persistence for sites on the positive or negative half-lines. Here we show persistence of sites $m = 2$ and $m = -2$ on the log-log scale. We find that for $m = -2$ the behavior of persistence is determined only by the inverse power-law (21). On the other hand, for $m = 2$ the decrease of persistence is faster. Indeed, for positive m the behavior of persistence is dominated by the exponential decay (19) in the long-time limit. This is illustrated in the last plot, where we show persistence of site $m = 2$ on the log-scale.

V. CONCLUSIONS

In the present paper persistence of unvisited sites for two- and three-state quantum walks on a line was analyzed. We have found that in contrast to the classical random walk there is no connection between the asymptotic behavior of persistence and scaling of the variance with the number of steps. Concerning the two-state walk, we have analytically confirmed the numerical result obtained in [36] for the Hadamard walk. Moreover, we have extended the analysis to a one-parameter set of two-state quantum walks. In particular, we have shown that persistence of unvisited sites obeys an inverse power-law independent of the initial condition and the actual position of the site. The exponent of the inverse power-law is determined by the parameter of the coin operator.

The main result of the paper is the behaviour of persistence for three-state quantum walks. We have focused on a one-parameter family of walks which includes the familiar three-state Grover walk. Due to the trapping effect displayed by the considered set of quantum walks, the behaviour of persistence is more involved than for the two-state quantum walks. In particular, we have shown that the asymptotic scaling of persistence is in general determined by a combination of an inverse power-law and an exponential decay. However, both the exponent of the inverse power-law and the decay rate of the exponential decline depend on the initial coin state. Therefore, it is possible to obtain various asymptotic regimes of persistence by choosing proper initial conditions. Moreover, one can employ the asymmetry of the trapping effect to achieve different asymptotic scaling of persistence for sites on the positive and negative half-line. All obtained results have been facilitated by using a suitable basis formed by the eigenvectors of the coin operator. This allows to express persistence in closed and compact form and trace back the ways it is influenced by the initial state and its coherence.

The present study is limited to the quantum walks on a line. A natural extension is to consider persistence of unvisited sites in quantum walks on higher-dimensional lattices. It would be interesting if similar effects, such as

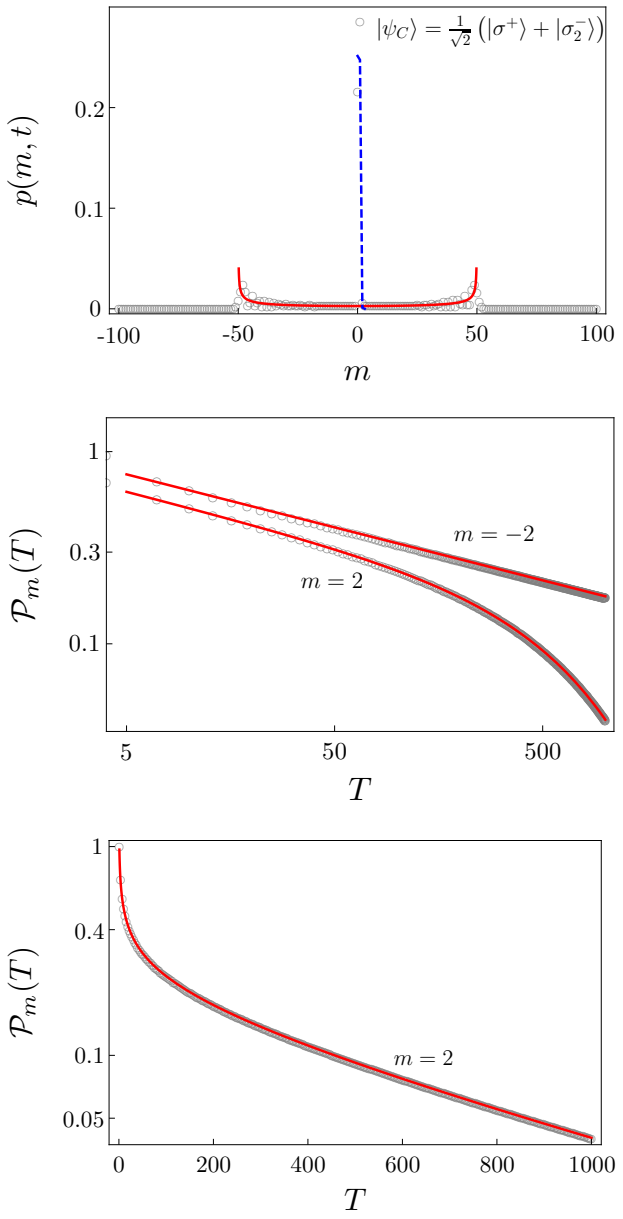

FIG. 7. Probability distribution and persistence for the three-state walk starting with the coin state (18). The coin parameter was chosen as $\rho = 0.5$. In the upper plot we display the probability distribution after $t = 100$ steps. Note that the trapping probability is non-zero only on the positive half-line. The lower plot shows persistence of sites $m = 2$ and $m = -2$ on the log-log scale. For $m = -2$ the behavior of persistence is determined only by the inverse power-law (21). However, for $m = 2$ the decrease of persistence is exponential (19), as we illustrate in the last plot with the logarithmic scale.

the dependency of persistence on the initial condition and various regimes of persistence for different lattice sites, can be found on more complicated lattices.

ACKNOWLEDGMENTS

We appreciate the financial support from RVO 68407700. MŠ is grateful for the financial support from GAČR under Grant No. 14-02901P. IJ is grateful for the financial support from GAČR under Grant No. 13-33906S.

Appendix A: Integral $\mathcal{I}_m(T)$ for a two-state walk

We dedicate this appendix to evaluating integral $\mathcal{I}_m(T)$ defined in (3) for the two-state walk. The limit density $w(v)$ is given by the formula (6). Since the limit density (6) is non-zero only for $|v| \leq \rho$, we replace the lower bound in the integral (3) with $|m|/\rho$. With the substitution $u = \frac{m}{\rho t}$ we rewrite $\mathcal{I}_m(T)$ into the form

$$\mathcal{I}_m(T) = \frac{\sqrt{1-\rho^2}}{\rho\pi} \int_{\frac{|m|}{\rho T}}^{1} \frac{1 - \mathrm{sgn}(m) u (2|h_+|^2 - 1)}{u\left(1-\rho^2 u^2\right)\sqrt{1-u^2}} du.$$

Evaluating the integral we obtain

$$\mathcal{I}_m(T) = \frac{\sqrt{1-\rho^2}}{\rho\pi}\ln\left(\frac{\rho T}{|m|}\left(1+\sqrt{1-\frac{m^2}{\rho^2T^2}}\right)\right) + \frac{1}{\pi}\arctan\left(\frac{\rho}{\sqrt{1-\rho^2}}\sqrt{1-\frac{m^2}{\rho^2T^2}}\right) + \\ +\mathrm{sgn}(m)\frac{2|h_+|^2-1}{\rho}\left(\frac{1}{\pi}\arctan\left(\frac{|m|}{\rho T}\sqrt{\frac{1-\rho^2}{1-\frac{m^2}{\rho^2T^2}}}\right)-\frac{1}{2}\right).$$

Moreover, for large number of steps T this function tends to

$$\mathcal{I}_m(T) \approx \frac{\sqrt{1-\rho^2}}{\rho\pi}\ln\left(\frac{2\rho T}{|m|}\right) - \frac{\arcsin\rho}{\pi} + \mathrm{sgn}(m)\frac{2|h_+|^2-1}{2\rho}.$$

Therefore, for large T the function $\mathcal{I}_m(T)$ grows like a logarithm

$$\mathcal{I}_m(T) \sim \lambda\ln\left(\frac{T}{|m|}\right),$$

where the pre-factor reads

$$\lambda = \frac{\sqrt{1-\rho^2}}{\rho\pi}.$$

Appendix B: Integral $\mathcal{I}_m(T)$ for a three-state walk

In this appendix we evaluate the integral (3) for a three-state quantum walk, i.e. the limit density is given by (10). Using the substitution $u = \frac{m}{\rho t}$ we rewrite $\mathcal{I}_m(T)$ into the form

$$\mathcal{I}_m(T) = \frac{\sqrt{1-\rho^2}}{\rho\pi}\int\limits_{\frac{|m|}{\rho T}}^{1}\frac{1-|g_2|^2-(g_1\overline{g_2}+\overline{g_1}g_2)u+(|g_2|^2-|g_+|^2)u^2}{u(1-u^2)\sqrt{1-u^2}}du.$$

Evaluating the integral we obtain the following result

$$\mathcal{I}_m(T) = \frac{\sqrt{1-\rho^2}}{\pi\rho}\left(1-|g_2|^2\right)\left(\ln\left(\frac{\rho T}{|m|}\right)+\ln\left(1+\sqrt{1-\frac{m^2}{\rho^2T^2}}\right)\right) - \\ -\frac{1}{2\pi}\left(1-|g_2|^2\right)\arctan\left(\frac{2\rho\sqrt{\left(1-\frac{m^2}{\rho^2T^2}\right)(1-\rho^2)}}{\left(2-\frac{m^2}{\rho^2T^2}\right)\rho^2-1}\right)+\frac{1}{\pi\rho^2}\left(|g_2|^2-|g_+|^2\right)\arctan\left(\rho\sqrt{\frac{1-\frac{m^2}{\rho^2T^2}}{1-\rho^2}}\right) - \\ -\frac{1}{2\pi\rho}\left(\overline{g_1}g_2+g_1\overline{g_2}\right)\left(\pi-2\arctan\left(\frac{\frac{|m|}{\rho T}\sqrt{1-\rho^2}}{\sqrt{1-\frac{m^2}{\rho^2T^2}}}\right)\right).$$

For large number of steps T this function approaches

$$\mathcal{I}_m(T) \approx \frac{\sqrt{1-\rho^2}}{\pi\rho}\left(1-|g_2|^2\right)\ln\left(\frac{2\rho T}{|m|}\right)+\frac{1}{2\pi}\left(1-|g_2|^2\right)\arctan\left(\frac{2\rho\sqrt{1-\rho^2}}{1-2\rho^2}\right)+ \\ +\frac{1}{\pi\rho^2}\left(|g_2|^2-|g_+|^2\right)\arctan\left(\rho\sqrt{\frac{1}{1-\rho^2}}\right)-\frac{1}{2\rho}\left(\overline{g_1}g_2+g_1\overline{g_2}\right)$$

Wee see that $\mathcal{I}_m(T)$ asymptotically grows like a logarithm

$$\mathcal{I}_m(T) \sim \lambda\ln\left(\frac{T}{|m|}\right),$$

where the pre-factor reads

$$\lambda = \frac{\sqrt{1-\rho^2}}{\pi\rho}\left(1-|g_2|^2\right).$$

[1] Y. Aharonov, L. Davidovich and N. Zagury, Phys. Rev. A **48**, 1687 (1993).
[2] D. Meyer, J. Stat. Phys. **85**, 551, (1996).
[3] E. Farhi and S. Gutmann, Phys. Rev. A **58**, 915 (1998).
[4] N. Shenvi, J. Kempe and K. Whaley, Phys. Rev. A **67**, 052307 (2003).
[5] A. M. Childs and J. Goldstone, Phys. Rev. A **70**, 022314 (2004).
[6] V. Potoček, A. Gabris, T. Kiss and I. Jex, Phys. Rev. A **79**, 012325 (2009).
[7] A. M. Childs and Y. Ge, Phys. Rev. A **89**, 052337 (2014).
[8] J. K. Gamble, M. Friesen, D. Zhou, R. Joynt and S. N. Coppersmith, Phys. Rev. A **81**, 052313 (2010).
[9] S. D. Berry and J. B. Wang, Phys. Rev. A **83**, 042317 (2011).
[10] K. Rudinger, J. K. Gamble, M. Wellons, E. Bach, M. Friesen, R. Joynt and S. N. Coppersmith, Phys. Rev. A **86**, 022334 (2012).
[11] M. Hillery, D. Reitzner and V. Bužek, Phys. Rev. A **81**, 062324 (2010).
[12] M. Hillery, H. J. Zheng, E. Feldman, D. Reitzner and V. Bužek, Phys. Rev. A **85**, 062325 (2012).
[13] S. Cottrell and M. Hillery, Phys. Rev. Lett. **112**, 030501 (2014).
[14] V. M. Kendon and C. Tamon, J. Comput. Theor. Nanosc. **8**, 422 (2011).
[15] P. Kurzynski and A. Wojcik, Phys. Rev. A **83**, 062315 (2011).
[16] K. E. Barr, T. J. Proctor, D. Allen and V. M. Kendon, Quantum Inf. Comput. **14**, 417 (2014).
[17] X. Zhan, H. Qin, Z. H. Bian, J. Li and P. Xue, Phys. Rev. A **90**, 012331 (2014).
[18] I. Yalcinkaya and Z. Gedik, J. Phys. A **48**, 225302 (2015).
[19] A. M. Childs, Phys. Rev. Lett. **102**, 180501 (2009).
[20] N. B. Lovett, S. Cooper, M. Everitt, M. Trevers and V. Kendon, Phys. Rev. A **81**, 042330 (2010).
[21] E.W. Montroll, in *Random Walks on Lattices*, edited by R. Bellman (American Mathematical Society, Providence, RI), Vol. **16**, 193 (1964).
[22] G. Pólya, Mathematische Annalen **84**, 149 (1921).
[23] M. Štefaňák, I. Jex and T. Kiss, Phys. Rev. Lett. **100**, 020501 (2008).
[24] M. Štefaňák, T. Kiss and I. Jex, Phys. Rev. A **78**, 032306 (2008).
[25] N. Inui, Y. Konishi and N. Konno, Phys. Rev. A **69**, 052323 (2004).
[26] N. Inui, N. Konno and E. Segawa, Phys. Rev. E **72**, 056112 (2005).
[27] N. Inui and N. Konno, Physica A, **353**, 133 (2005).
[28] S. Falkner and S. Boettcher, Phys. Rev. A **90**, 012307 (2014).
[29] K. Watabe, N. Kobayashi, M. Katori and N. Konno, Phys. Rev. A **77**, 062331 (2008).
[30] T. Kiss, L. Kecskes, M. Štefaňák and I. Jex, Phys. Scr. **T135**, 014055 (2009).
[31] A. Ambainis, E. Bach, A. Nayak, A. Vishwanath and J. Watrous, in *Proceedings of the 33th STOC*, ACM New York, p. 60 (2001).
[32] F. A. Grünbaum, L. Velázquez, A. H. Werner and R. F. Werner, Commun. Math. Phys. **320**, 543 (2013).
[33] P. Sinkovicz, Z. Kurucz, T. Kiss and J. K. Asbóth, Phys. Rev. A **91**, 042108 (2015).
[34] J. Bourgain, F. A. Grünbaum, L. Velázquez and J. Wilkening, Commun. Math. Phys. **329**, 1031 (2014).
[35] S. Chandrasekhar, Rev. Mod. Phys. 15, 1 (1943)
[36] S. Goswami, P. Sen, and A. Das, Phys. Rev. E **81**, 021121 (2010).
[37] M. Štefaňák, I. Bezděková and I. Jex, Eur. Phys. J. D **66**, 142 (2012).
[38] T. Machida, Quantum Inf. Comp. **15**, 0406 (2015).
[39] M. Štefaňák, I. Bezděková and I. Jex, Phys. Rev. A **90**, 012342 (2014).
[40] G. Grimmett, S. Janson and P. F. Scudo, Phys. Rev. E **69**, 026119 (2004).
[41] A. Kempf and R. Portugal, Phys. Rev. A **79**, 052317 (2009).
[42] N. Konno, Quantum Inf. Process. **1**, 345 (2002).
[43] N. Konno, J. Math. Soc. Jpn. **57**, 1179 (2005).
[44] M. Štefaňák, S. M. Barnett, B. Kollár, T. Kiss and I. Jex, New J. Phys. **13**, 033029 (2011).